UNIVERSITY OF PÉCS
FACULTY OF SCIENCES
INSTITUTE OF CHEMISTRY

Photochemical water-splitting reaction catalyzed by Ce(III) ions

Supervisor: Dr. Katalin Ősz
associate professor

Author: Simona Jankova
BSc in Chemistry

PÉCS 2023

Table of Contents

1. Introduction 4

2. Literature Background 5

2.1. Experimental Evidence for the Production of Hydrogen in the Ce(III) Catalyzed Photochemical Reduction of Water[16] 8

2.2. The Aqueous Electrochemistry of Cerium 10

2.3. Redox Properties of Cerium Ions 11

2.4. Representation of the different photochemical and photophysical processes on Jablonski diagrams 12

2.5. Actinometry 14

2.5.1. Ferrioxalate actinometry 15

3. Experimental methods 16

3.1. Reagents used. 16

3.2. Measurement Methods 18

3.2.1. Scanning Spectrophotometer 18

3.2.2. Diode Array Spectrophotometer 19

3.2.3. PhotoCube Photoreactor 20

4. Results and Discussion 22

4.1. Calibration of the PhotoCube photoreactor using actinometry 22

4.2. Calibration of the diode array spectrophotometer 24

4.3. Ce(III) catalyzed water-splitting kinetics in PhotoCube 29

4.3.1. Reaction with mass measurements 29

4.3.2. Effect of changing the Ce(III) concentration 34

4.4. Kinetics of the Ce(IV)+H_2O reaction in the diode array spectrophotometer 36

5. Summary 40

6. Acknowledgment 42

7. References 43

1. Introduction

The production of clean and renewable energy is essential for addressing the challenges of climate change and global energy demands. Photochemical water-splitting is one promising approach for producing hydrogen as a sustainable solar energy fuel. This process involves the use of light to drive the decomposition of water into oxygen and hydrogen gases. Ce(III) ions are effective catalysts for photochemical water-splitting, as they can facilitate the transfer of electrons between water molecules and generate reactive intermediates that promote the overall reaction. Homogeneous reactions catalyzed by Ce(III) ions have been extensively studied due to their unique redox properties and ability to participate in various chemical transformations. These photocatalysts and photo-sensitive molecules play a crucial role in the reaction by absorbing light and generating reactive intermediates that facilitate the overall response. By carefully selecting and optimizing these materials, the efficiency and selectivity of the reaction can be improved. Photochemistry provides a means of converting solar energy into valuable chemical energy, which can be used for various applications such as fuel production, pharmaceutical synthesis, and environmental remediation. A key advantage of photochemical reactions is the ability to activate specific chemical bonds selectively and generate reactive intermediates under mild conditions.

In recent years, significant progress has been made in developing new photochemical systems that can efficiently convert solar energy into chemical energy. These include new photocatalysts, photoelectrochemical cells, and photovoltaic devices. These advances have led to a greater understanding of the fundamental principles underlying photochemistry and the development of new technologies for harnessing solar energy.

2. Literature Background

Since the 1950s,[1] it has been recognized that aqueous cerium(III) and cerium(IV) complexes exhibit light sensitivity, an exceptional property among lanthanide ions. Cerium is also distinguished from other lanthanides by its oxidation state of +4, which remains relatively stable in an aqueous environment. Researchers have investigated the photooxidation of water by cerium(IV),[2,3,4] and the impact of certain additives, such as thallium(I) ions.[5] Earlier, there was interest in exploiting cerium(IV) photochemistry to facilitate organic transformations of carboxylic acids,[6,7] alcohols,[7] and oxo compounds.[8] However, it is essential to note that despite discussing the photoactivity of both oxidation states of cerium together, the origins of light absorption in the two systems differ significantly. Cerium(III) complexes exhibit f-f transitions, whereas cerium(IV) complexes do not possess f electrons, they typically show intense charge transfer bands.

In the 21st century, there has been a significant increase in interest in cerium photocatalysis. This includes various inorganic processes, such as sulfur(IV) autoxidation,[9] peroxomonosulfate ion[10] and singlet oxygen[11] reactions, and hydrogen production. Additionally, several studies have reported using different cerium forms to enhance the degradation of organic pollutants.[12,13] Most of these applications focus on selective organic reactions, such as aryl coupling reactions, functionalization of alkanes, dehydroxymethylation of alcohols, decarboxylative hydrazination, selective C-C bond scission of ketones, decarboxylative oxygenation, and lactonization. Furthermore, a general strategy has been proposed to improve the overall efficiency of cerium photocatalysis. Recently, these developments have been referred to as a "renaissance of ligand-to-metal charge transfer by cerium photocatalysis."[14]

When measuring pure cerium(IV) solutions using spectrophotometry, interference from cerium(III) contamination is reduced because the molar absorptivity values of cerium(IV) are at least four times higher than those of cerium(III) at every wavelength.

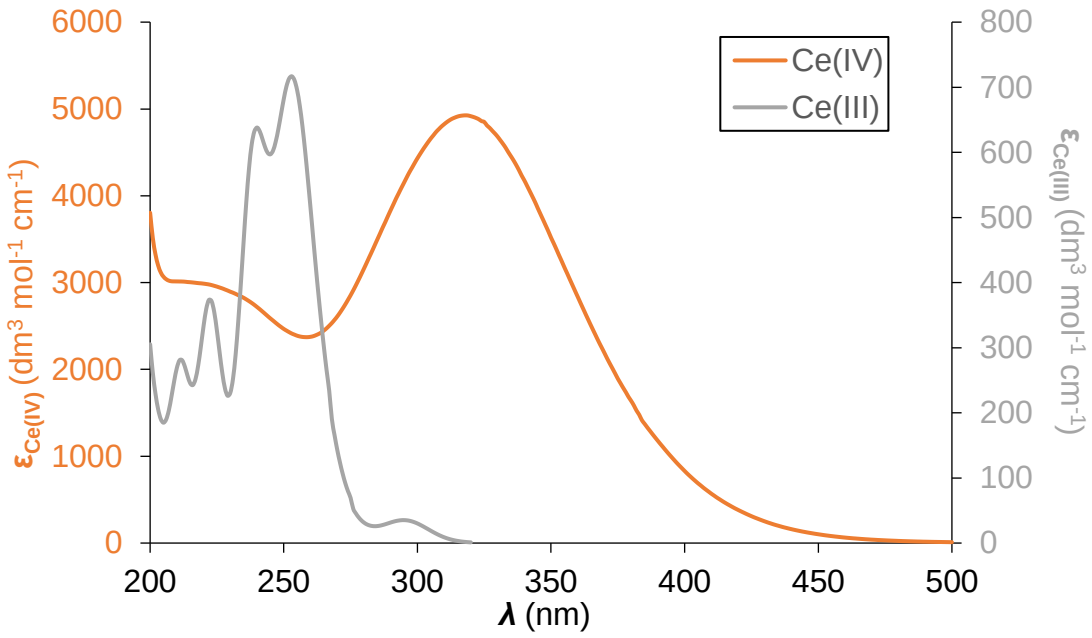

Figure 1: UV-vis molar absorptivity values of aqueous Ce(III) and Ce(IV) solutions in $c(H_2SO_4)$ = 0.5 mol dm^{-3}. Data from the literture.[14]

A proposed scheme for the photochemical oxidation of water in photosynthesis agrees with previously reported data. Weiss, Porret, and Baur[2] conducted early investigations into photooxidation by ceric ions. Heidt and Smith[1] conducted a more detailed study, assuming the formation of an active ceric dimer deactivated by cerous ions. Spectrophotometric measurements suggest no dimer formation and that most ceric ions exist as the ion-pair complex Ce^{4+} OH^{-} in ceric perchlorate solutions. Heidt and Smith's kinetic results[1] can be explained using a reaction scheme that involves the ion-pair complex as the active species for the primary electron-transfer excitation step. This scheme can also explain why the quantum yield is much smaller for ferric ions, making it difficult to measure under standard laboratory conditions.[15]

(1) $$Ce^{4+}\ OH^{-} \underset{k_d}{\overset{k_\epsilon I}{\rightleftharpoons}} Ce^{3+}\ OH^{-}$$

(2) $$Ce^{3+}\ OH \xrightarrow{k_s} Ce^{3+} + OH$$

(3) $$Ce^{3+}\ OH \xrightarrow{k_0} Ce^{4+} + OH^{-}$$

(4) $$Ce^{4+}\ OH^{-} + OH \xrightarrow[\text{OH radical a reducing species!}]{k_0} Ce^{3+} + H_2O_2$$

(5) $$2\,Ce^{4+}OH^{-} + H_2O_2 \xrightarrow[\text{not rate determining}]{} 2\,HOH + 2\,Ce^{3+} + O_2\uparrow$$

(6) $$[Ce^{3+}OH] = \frac{k_\epsilon I}{k_d + k_s}$$

(7) $$[OH] = \frac{k_\epsilon k_s I}{(k_d + k_s)(k_0\,[Ce^{3+}] + k_2\,[Ce^{4+}OH^{-}])}$$

Scheme 1: Describing different results obtained by a variety of scientists.

(1) Photochemical oxidation of water in understanding the process of photosynthesis; (2) Weiss and Porret photo-oxidation by ceric ions; (3) Qualitative effect of the previous photo-oxidation made by Baur (1908); (4) Detailed study done by Heidt and Smith; (5) Photo-initiated polymerization, Obtained formulas from stationary-state kinetics: (6) Photo-initiated polymerization; (7) Oxidation[15]

For a while, it has been known that the photochemical reduction of ceric to cerous ions in dilute aqueous perchloric acid is accompanied by oxygen evolution and inhibited by cerous ions. The cerous ion's effect is attributed to the inner filter effect, photon deactivation of excited ceric ions, and cerous ion light absorption leading to ceric ion oxidation. Research has shown that the photochemical oxidation of cerous to ceric ions can produce hydrogen. In contrast, irradiation of an aqueous solution of cerous and ceric perchlorates can produce hydrogen and oxygen under certain conditions. By manipulating the concentration of acid and cerous ions, an aqueous solution containing both ceric and cerous ions can alternately produce pure oxygen in darkness and almost pure hydrogen in light or both gases simultaneously. An article written about a study of the influence of acid and cerous ion concentration on the photochemical oxidation of cerous ions at 25 °C by the light of 2537 Å, evaluating the maximum possible quantum yield of the reaction in this system and the reactions by which light absorbed by cerous ions photochemically reduce water. Additional evidence shows that

hydrogen can be produced by the photochemical reduction of water by light absorbed by cerous ions.[16]

2.1. Experimental Evidence for the Production of Hydrogen in the Ce(III) Catalyzed Photochemical Reduction of Water[16]

An experiment done in 1954[16] discovered new evidence showing that hydrogen can be produced by shining light on a mixture of cerous perchlorate and perchloric acid. The experiment was conducted by making a solution containing perchloric acid and cerous perchlorate and then exposing it to light. Then a small amount of gas was collected, produced by the reaction, and found to contain hydrogen. The gas ignited, and it was found that it had water vapour. Also, the reaction produced ceric ions.

Forward Reactions:

$$Ce{\cdot}H_2O^{+3} + h\nu = {}^*Ce{\cdot}H_2O^{+3} \quad (1)$$

$${}^*Ce{\cdot}H_2O^{+3} + H_3O^+ = Ce{-}OH{-}H_2^{+4} + H_2O \quad (2)$$

$$Ce{-}OH{-}H_2^{+4} + Ce{\cdot}H_2O^{+3} = 2CeOH^{+3} + H_2 + H^+ \quad (3)$$

The sum of reactions 1, 2 and 3 is $2Ce{\cdot}H_2O^{+3} + h\nu = 2CeOH^{+3} + H_2$

Quenching Reactions:

$${}^*Ce{\cdot}H_2O^{+3} = Ce{\cdot}H_2O^{+3} + \text{heat} \quad (1')$$

$${}^*Ce{\cdot}H_2O^{+3} + H_3O^+ = Ce{\cdot}H_2O^{+3} + H_3O^+ + \text{heat} \quad (2')$$

$$Ce{-}OH{-}H_2^{+4} + H_2O = Ce{\cdot}H_2O^{+3} + H_3O^+ + \text{heat} \quad (3')$$

Scheme 2: The set of reactions for the photochemical reduction of water by cerous ions.[16]

Reaction (1) represents that light absorbed by cerous ions initiates the reaction. Reactions (2) and (1') account for the observed dependence of l/ϕ^* and upon $1/[H^+]$. The terms containing $[H^+]$ would be negligible if reaction (2) took place, but reaction (1') and, consequently, k_1' were insignificant. Reactions (3) and (3') account for the observed dependence of l/ϕ^* upon $1/[Ce^{3+}]$. The terms containing $[Ce^{3+}]$ would be negligible if reaction (3) took place, but reaction (3') and consequently k_3' were insignificant. Reaction (2') accounts for the fact that l/ϕ^* does not equal 1/2 by extrapolation when both $1/[H^+]$ and $l/[Ce^{3+}]$ are equal to zero. The constant ***a*** would be equal to 1/2 if reaction (2') and consequently k_2' was negligible.

The above reactions give the following mathematical relationships between ϕ* and the components of the system:

I. $\phi^* = d(Ce^{IV})/I dt = 2k_3(Ce\text{–}OH\text{–}H_2{}^{+4})(Ce^{+3})/I$
where I represents light absorbed by cerous ions per unit time per unit volume.

II. $d(*Ce^{+3}\cdot H_2O)/dt = I = k_2(*Ce^{+3}\cdot H_2O)(H^+) + k_1'(*Ce^{+3}\cdot H_2O) + k'_2(*Ce^{+3}\cdot H_2O)(H^+) = -d(*Ce^{+3}\cdot H_2O)/dt$; hence $(*Ce^{+3}\cdot H_2O) = I/[k_1' + (k_2 + k_2')(H^+)]_1$.

III. $d(Ce\text{–}OH\text{–}H_2{}^{+4})/dt = k_2(*Ce^{+3}\cdot H_2O)(H^+) = k_3(Ce\text{–}OH\text{–}H_2{}^{+4})(Ce^{+3}) + k_3'(Ce\text{–}OH\text{–}H_2{}^{+4}) = -d(Ce\text{–}OH\text{–}H_2{}^{+4})/dt$; hence $(Ce\text{–}OH\text{–}H_2{}^{+4}) = (*Ce^{+3}\cdot H_2O)k_2(H^+)/[k_3' + k_3(Ce^{+3})]_2 = Ik_2(H^+)/[\ ]_1[\ ]_2$.

Scheme 3: Set of reactions accounts quantitatively for the influence of variations in the concentrations of perchloric acid and cerous perchlorate upon the quantum yield, (ϕ*).[16]

Developing efficient and sustainable strategies for converting solar energy into chemical fuels is a significant research challenge in renewable energy.[17] One promising approach is the photocatalytic splitting of water into hydrogen and oxygen,[18] which requires suitable catalysts to drive the necessary redox reactions. The initial phase of the catalytic cycle, which involves water oxidation by cerium(IV), can be facilitated by light or different types of heterogeneous catalysts, such as ruthenium dioxide. The formation of hydrogen gas, the other half of the reaction, also requires an energy source such as light. According to the previous literature, this step can also be catalyzed. When choosing a catalyst for these two steps, metal complexes with non-easily oxidizable organic ligands should be preferred due to the strong oxidizing property of cerium(IV). One example of such an agent is the ruthenium(III) aqua ion, although it is important to note that catalysts with organic ligands can still be used. For instance, the tris-bipyridyl complex of ruthenium(II) can be used since it is stable enough to protect bipyridyl from rapid oxidation by cerium(IV). Other possible ligands for the catalyst include tetra-amido macrocyclic ligands (TAML). Furthermore, several known cerium(III) complexes (including functionalized macrocycles as ligands) exhibit photochemical activity in aqueous solutions. The expectations are to modify the cerium(III)/cerium(IV) redox potentials and prevent cerium(III) and cerium(IV) from hydrolysis under mildly acidic conditions by using these

ligands. This would allow less corrosive media for cerium(III)-catalyzed water-splitting via sunlight.

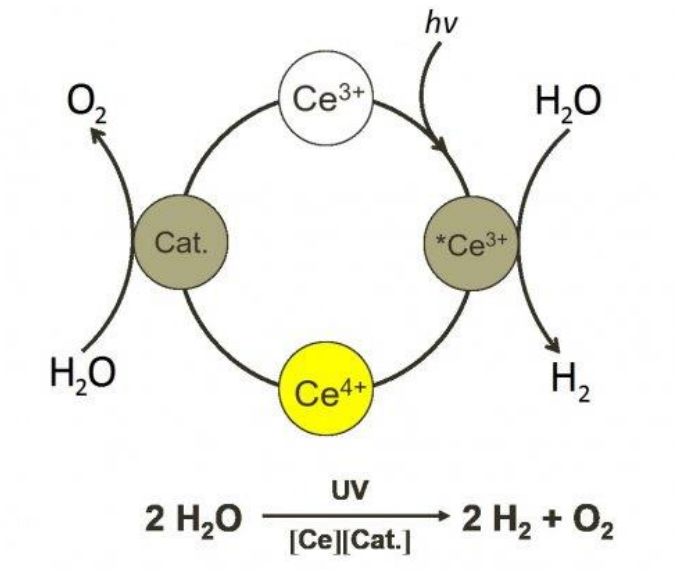

Figure 2: Catalytic cycle: first half-reaction is the oxidation of water by cerium(IV) which can be catalyzed by light or various heterogenic catalysts (e.g., ruthenium dioxide). The other half-reaction, the formation of hydrogen gas, requires light or other energy sources to take place.

2.2. The Aqueous Electrochemistry of Cerium

In general, the Ce(III)/Ce(IV) redox reaction is characterized by several factors. [19] First, there is a charge transfer that occurs through multiple steps. Second, the anodic and cathodic charge transfer coefficients have different values. Last, the behaviour of the reaction is highly influenced by coordination with ligands. Although the reaction is relatively fast, the reduction process is slower than the oxidation, and the voltammograms are irreversible in many acid media. Additionally, oxygen evolution can make it difficult to define an oxidation peak in some cases, such as in MSA and sulfuric acid. [20] The interaction with ligands significantly affects the cerium redox reaction's thermodynamic and kinetic parameters. Ligands can cause a shift in the standard electrode potential of the reaction, and changes in the coordination sphere at the electrode surface can lead to a more positive electrode potential. The larger size of the coordination and solvation sphere reduces the diffusion coefficient of cerium ions, making the reaction less reversible and more dependent on mass transport.

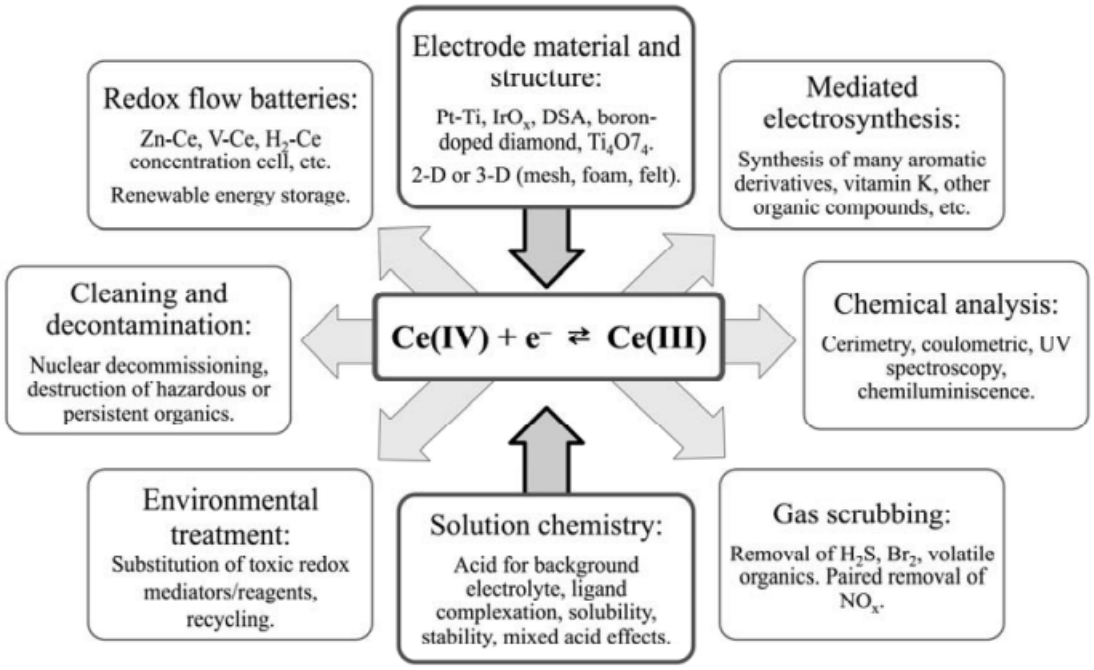

Figure 3: Wide range of use of the pair Ce(III)/Ce(IV) in everyday life.[20]

2.3. Redox Properties of Cerium Ions

As the most abundant rare-earth metal on Earth, constituting approximately 0.0046 wt% of the Earth's crust, cerium plays a crucial role in various industries. One of the most well-known compounds of cerium is cerium dioxide, or ceria, which is renowned for its distinctive redox properties and remarkable oxygen mobility. Due to these characteristics, ceria is a potent oxidant extensively used in catalysis and medicine. However, the significance of ceria-based materials is not limited to these fields alone. These materials also play a central role in energy devices such as fuel cells, where their exceptional oxygen storage and release capabilities make them highly valuable. Furthermore, the automotive industry relies heavily on ceria, a vital component in three-way catalysts present in exhaust systems. In conclusion, cerium, and its compounds, especially ceria, have far-reaching industrial applications, making them essential in several fields.[21]

The survey shows that the electronic environment provided by the coordination sphere around a cerium ion can significantly affect its oxidizing or reducing ability. The range of cerium(IV) reduction potential is extensive and can vary greatly depending on whether the solution is aqueous or non-aqueous. Therefore, while cerium(IV) is often regarded as a strong oxidant, cerium(III) can be a potent reductant due to the influence of its coordination environment.[19]

Some unique aspects of cerium redox chemistry: cerium remains a complex cation in its +3 and +4 oxidation states. It is best stabilized by hard anions that stabilize cerium(IV) complexes most significantly. Additionally, the change from f1 to f0 configuration upon oxidation from the trivalent to tetravalent state results in a change in ionic radius, a distinctive feature of cerium compared to transition metals. Covalent bonding plays a minor role in shaping the coordination sphere of cerium complexes during oxidation reactions, and sizeable inner sphere reorganization energies are expected. This implies that thermodynamic considerations alone may not provide predictive power in cerium oxidation reactions.[19]

Using the cerium redox couple in solution has many practical applications.[20] Ce(IV) can fully oxidize organic compounds to CO_2 in closed acidic systems as a potent oxidizing agent. This has been tested successfully in a pilot plant for wastewater treatment. In organic chemistry,[22] it acts as a redox mediator for various reactions. It has industrial significance, such as in the oxidation of naphthalene to naphthoquinone at a 100-ton-per-year scale and the synthesis of vitamin K3 at a 400-ton-per-year scale. Additionally, it has proven helpful for gas scrubbing, with removal efficiencies of 95%, 45%, and 100% demonstrated for harmful gases like H_2S, NO_x, and SO_2, in order. Due to its many applications, recycling, and regenerating cerium (e.g., through electrochemical methods) has become increasingly important for economic and ecological reasons.

2.4. Representation of the different photochemical and photophysical processes on Jablonski diagrams

Scheme 4 illustrates that when photons with energy $h\nu = hc/\lambda$ are absorbed by the chromophore C, they can be raised from their ground electronic state to an excited singlet state C*. This occurs if the photon energy is greater than the threshold energy, which is the energy difference

between the first excited state of C and its ground state. The excited state C* has excess vibrational energy or maybe in a higher electronic state and is considered "hot". At this stage, the excited state is not in thermal equilibrium with the surrounding medium.[24]

$$\mathrm{C} + h\nu \rightarrow \mathrm{C}^{*}\,(\mathrm{hot})$$

$$\mathrm{C}^{*}\,(\mathrm{hot}) \rightarrow \mathrm{C}^{*}\,(\mathrm{thermalized}) \ \text{ or } \ \mathrm{S}_1\,(\mathrm{thermalized})$$

$$\mathrm{S}_1\,(\mathrm{thermalized}) \rightarrow \mathrm{S}_0 + \mathrm{heat}\,(\mathrm{internal\ conversion}) \quad k_{\mathrm{IC}}$$

$$\mathrm{S}_1\,(\mathrm{thermalized}) \rightarrow \mathrm{S}_0 + h\nu_{\mathrm{f}}\,(\mathrm{fluorescence}) \quad k_{\mathrm{f}}$$

$$\mathrm{S}_1\,(\mathrm{thermalized}) \rightarrow \mathrm{T}_1\,(\mathrm{thermalized})\,(\mathrm{intersystem\ crossing}) \quad k_{\mathrm{T}}$$

$$\mathrm{S}_1\,(\mathrm{thermalized}) \rightarrow \mathrm{P}\ (\mathrm{photochemical\,step}) \quad k_{\mathrm{photochem}}$$

Scheme 4: 6 reactions where C(chromophore) is raised from the ground electronic state(S_0) to an excited singlet state C* (one of the S_1, S_2, …singlet excited states); C*(hot) thermalizes, in the sense that it loses its excess energy as the heat transferred to the surrounding medium forming the S_1(thermalized) state. The S_1 state can decay in one of four ways (k_{IC}, k_f, k_T, $k_{photochem}$).[24]

Within a few femtoseconds (fs), C*(hot) loses its excess energy as heat to the surrounding medium and becomes the S_1(thermalized) state, which is in thermal equilibrium with the environment. The S_1(thermalized) state has four ways to decay: (1) Internal conversion (IC) can convert the excess energy to heat and decay to the ground state with a rate constant k_{IC}. (2) By fluorescence, it can emit a photon of energy $h\nu_f$ and decay to the ground state S_0 with a rate constant k_f. (3) By intersystem crossing (ISC), it can change the electron spin and form a thermalized triplet state T_1 (thermalized) with a rate constant k_T. (4) It can react photochemically to form the product P with a first-order rate constant $k_{photochem}$.

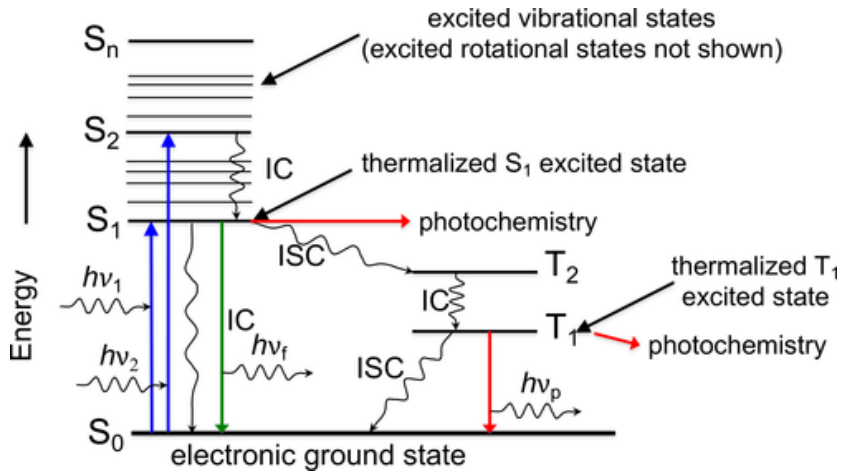

Figure 4: Energy-level diagram of the ground and excited states [singlet (S) and triplet (T)] of the chromophore C. The internal processes are internal conversion (IC) and intersystem crossing (ISC). Light emission can occur as fluorescence ($h\nu_f$) or phosphorescence ($h\nu_p$) [adapted from Bolton et al.[23]]

2.5. Actinometry

Actinometry uses a chemical reaction to measure the intensity of electromagnetic radiation, particularly ultraviolet radiation from the sun. It involves using a substance that reacts in a known way to radiation to determine the amount or intensity of radiation present. Actinometers[24] are tools used to measure the number of photons in each area. There are two types of actinometers - physical and chemical. Chemical actinometers are photochemical systems with a predetermined quantum yield, making them helpful in determining precise photon fluxes for photochemical reactions.

Every chemical actinometer requires a photochemical reaction that must follow the principles and laws of photochemistry and other applicable regulations. For an actinometer to be trustworthy and precise, it's essential to know its quantum yield accurately. Once the quantum yield is determined for a few standardized actinometers, it can serve as a secondary reference for determining the quantum yield of other actinometers. This can be achieved by using the same equipment and light sources to measure the chemical yield of the chosen actinometer and comparing it against the chemical yield of one of the standardized actinometers.

2.5.1. Ferrioxalate actinometry

One of the substances used in my measurements was potassium-[tris(oxalato)-ferrate(III)]-trihydrate, which I employed as an actinometer by using its photoreduction. This method, first introduced by C.G. Hatchard and C.A. Parker in 1956[25] and approved by IUPAC, detailed measurements in the range of 250-500 nm. The bright green octahedral complex contains iron in the +3-oxidation state. As the complex is light-sensitive, it is necessary to store it in the dark and to ensure that the reaction mixture is constantly mixed during the measurement to avoid any inconsistency.

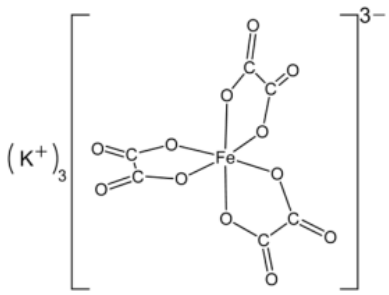

$$2[Fe(C_2O_4)_3]^{3-} \rightarrow 2[Fe(C_2O_4)_2]^{2-} + (COO)_2^{2-} + CO_2$$

Figure 5: Structural formula of potassium-[tris(oxalato)-ferrate(III)] and the stoichiometry of its photochemical reduction.

The complex anion decomposes in the solution phase under the influence of light in an acidic medium. The complex's central iron(III) ion is reduced to an iron(II) ion during the photocatalyzed process, while the oxalate ligand is oxidized to carbon dioxide. The quantum efficiency of the reaction is well known.

Potassium tris-oxalato-ferrate(III) trihydrate is an excellent chemical actinometer that can be applied for various purposes due to its ability to operate across a broad spectrum of wavelengths, making it more advantageous than uranyl oxalate, which was used previously. This compound possesses several desirable features, including high sensitivity, nearly a thousand times higher than uranyl oxalate, and high accuracy, especially under low light

conditions. Additionally, the photolyte and photolysis products exhibit outstanding stability, and the actinometer can function over an extensive range of intensities.

The quantity of Fe(II) produced was measured by spectrophotometry,[26] using o-phenanthroline to create a red-coloured complex called ferroin ($[Fe(phen)_3]^{2+}$), whose concentration can be measured by detecting absorbance at ~510 nm.

However, suppose actinometry is used to measure the light intensity of the spectrophotometer. In that case, there is no need for a separate spectrophotometric measurement to determine the amount of formed Fe(II), as the amount of Fe(II) produced can be calculated directly from the changes in the sample's spectrum by monitoring the concentration of the decomposed Fe(III) complex.

In my research, I conducted actinometric measurements based on a published article[26] by T. Lehóczki, É. Józsa, and K. Ősz, which further developed a previously described method. The original method involved measuring the amount of Fe(II) formed using complex formation with 2,2'-dipyridyl or phenanthroline, which was determined through spectrophotometry. In this method, Fe(II) ions react with phenanthroline to form the ferroin complex ($[Fe(phen)_3]^{2+}$), which has red colour, and its concentration can be determined by measuring the absorbance at 510 nm. Alternatively, the measurement can be performed with dipyridyl (bipy), where the Fe(II) ions form a red complex with dipyridyl ($[Fe(bipy)_3]^{2+}$), and the concentration of the complex can be determined by measuring the absorbance at 512 nm. The literature reports molar absorption coefficient values of 11000 dm^3/mol/cm for the $[Fe(phen)_3]^{2+}$ complex and 7200 dm^3/mol/cm for the $[Fe(bipy)_3]^{2+}$ complex.

3. Experimental methods

3.1. Reagents used.

Sigma Aldrich provided the solid compound cerium(III) chloride heptahydrate salt, with a trace metal basis of 99.9% and a molecular weight of 372.58 g/mol. The salt is soluble in alcohol, water, and acetone but only slightly soluble in tetrahydrofuran. It is hygroscopic and

air-sensitive, so it is stored under Argon. The salt was dissolved in different solvents, including water, perchloric acid, and sulfuric acid, to measure the catalytic reaction. Separate vessels containing only the solvents were also prepared. Initially, I used solutions with a concentration of $1.0 \cdot 10^{-4}$ mol/dm^3, which were later increased to $3.0 \cdot 10^{-4}$ mol/dm^3 to make it easier to monitor the photoreaction. Perchloric acid with a concentration of 1.0 mol/dm^3, which Ms. Ildikó Rapp-Kindner previously (07.09.2022.) prepared, was used.

Table 1: Different masses and concentrations for Ce(III) salt used on different occasions with two parallel measurements

Date:	Volume of solution (cm^3)	Mass of Ce(III)-less amount (g)	Mass of Ce(III)-more amount (g)	$c_{Ce(III)\text{-less}}$ (mol/dm^3)	$c_{Ce(III)\text{-more}}$ (mol/dm^3)
24.11.2022.	**500.0**	**0.06006**	**0.12317**	**$3.22 \cdot 10^{-4}$**	**$6.61 \cdot 10^{-4}$**
23.02.2023.	**45.0**	**0.00522**	**0.01544**	**$3.11 \cdot 10^{-4}$**	**$9.21 \cdot 10^{-4}$**
24.03.2023.	**200.0**	**0.02319**	**0.07419**	**$3.11 \cdot 10^{-4}$**	**$9.96 \cdot 10^{-4}$**

Another compound that I've used from Sigma Aldrich is cerium(IV) sulfate. This substance exists as a yellow powder and has a molecular weight of 332.24 g/mol. At a temperature of 25 °C, its density is 3.01 g/cm^3. I mixed the Ce(IV) powder with perchloric acid that had a concentration of 1.0 mol/dm^3. The amount of powder used was extremely small, specifically 0.00016612 g. The mass of the solid was measured with an analytical balance. The resulting sample had a volume of 2.5 cm^3. Its concentration was determined not only by the mass measurement but also from the spectrum measurement since the molar absorbance of Ce(IV) as a function of wavelength is known.

For actinometric measurements, the potassium-[tris(oxalato)-ferrate(III)]-trihydrate complex was prepared using a reaction between potassium oxalate and iron(III) chloride, following the methodology described in Dr. Béla Lengyel's book "General and Inorganic Chemical

Laboratory Practice." The complex was dissolved in 0.050 mol/dm^3 sulfuric acid, and solutions of 50.0 cm^3 were prepared by measuring 0.026-0.027 g of the complex. A 2.5 cm^3 solution was transferred into a 1.00 cm path-length quartz cuvette for measurement. Due to their sensitivity, the prepared solutions and complex were stored in the dark to prevent light-induced effects.

3.2. Measurement Methods

The analysis of the compounds is a pivotal component of this research. Therefore, the stock solutions prepared must undergo rigorous scrutiny using the PhotoCube photoreactor and Specord S 600 diode array spectrophotometer. The resulting data should be meticulously filtered and examined numerically and graphically using Microsoft Excel. Before conducting the measurements, actinometric analysis was performed using the previously described ferrate complex on both instruments. The kinetic curve, which is of paramount importance, must be evaluated using the initial rate method.

It is recommended to assess the precision of the outcomes using the SciDAVis software for scientific data analysis and visualization. The accuracy of the results can be determined by examining various parameters, including the standard deviation of the slope and intercept, the R^2 variance of the predicted values divided by the data variance as described by Gelman et al[27], and the utilization of χ^2 to test the null hypothesis H(0), which assumes no notable difference between the expected and observed data, according to J. Kwasiborski and M. Sobol.[28]

3.2.1. Scanning Spectrophotometer

The SPECORD 210 Plus is a double-beam spectrophotometer designed for advanced analysis in various applications. It offers high accuracy and reproducibility, a wide spectral range, and a fast scan speed. It features a user-friendly interface, easy-to-use software, and a variety of data export options. The instrument's compact and robust design makes it suitable for research and quality control laboratories. The SPECORD 210 Plus double-beam spectrophotometer is also used to accurately determine the concentrations of various dyes[29] in a solution, providing precise and reliable data for the research study. Spectrophotometers work by projecting a beam

of light onto a sample, then measuring the amount of transmitted light as a function of wavelength. Diode array spectrophotometers use a deuterium and a halogen lamp as the light source, and due to the relatively low sensitivity of the detector, the lamps have high intensity. Polychromatic light passes through the sample, meaning the monochromator is placed after the cuvette holder. Typically, the spectrum covers the range of 190-1100 nm. Direct measurement of light intensity indicates that the highest number of photons is obtained at shorter wavelengths, which can easily trigger photochemical reactions in light-sensitive and reactive substances. Thus, diode array spectrophotometers offer an excellent opportunity for studying photoinitiated reactions. To utilize diode array spectrophotometers as photoreactors, the number of photons passing through the sample must be determined through direct measurements or appropriate calibration methods. When spectrophotometers are used for photochemical studies, the excitation of photoactive substances and monitoring of the course of photochemical reactions coincide.

Some characteristics of the spectrophotometer:

1. Double beam optics for stable and accurate measurements
2. Wavelength range of 190-2500 nm for a wide range of applications
3. Fast scan speed of up to 2000 nm/min for quick data acquisition
4. High optical resolution for precise and detailed spectra
5. Built-in software with various data analysis tools and export options
6. User-friendly interface with a large colour touchscreen display
7. Compact and robust design for easy integration into laboratory workflows

3.2.2. Diode Array Spectrophotometer

Compared to a dispersive design, a diode array spectrophotometer uses a different type of single-beam optical design optimized for rapid, simultaneous acquisition of a full UV/Vis spectrum. The diffraction grating in a diode array instrument is located after the sample,

directly dispersing the transmitted light from the sample onto a diode array detector. Unlike a dispersive instrument, the grating in a diode array instrument does not move or scan. Instead, the transmitted light continuously illuminates the array detector, allowing for fast collection of spectral data. A unique feature of diode array instruments is using both source lamps simultaneously to illuminate the sample with all light wavelengths from 190 nm to 1100 nm.[30] The diode array detector, also known as a photodiode array detector (PDA), is a linear array of discrete photodiodes on a single integrated circuit (IC) chip. It is placed at the image plane from the grating to simultaneously detect a range of wavelengths. This detector is like an electronic version of a photographic digital camera detector array and is the key to fast spectral data collection in a diode array instrument. These instruments can collect a full range of UV/Vis spectrum in milliseconds to seconds, depending on the design, and are ideal for collecting complete spectral data on rapidly changing samples in fields such as kinetics, dissolution, liquid chromatography, and multicomponent analysis. Although subject to long-term drift, diode array instruments rarely experience issues since background corrections and sample data can be acquired in under a second. The diode array spectrophotometer used for my measurements was Analytik Jena Specord S 600. The SPECORD S 600 UV/Vis spectrophotometer offers laboratories the necessary precision and ease of use, speed, reliability, and exceptional optical capabilities. This high-performance diode array spectrophotometer operates with precision, speed, and simultaneity.

3.2.3. PhotoCube Photoreactor

The PhotoCube photoreactor manufactured by ThalesNano is a highly efficient and versatile device that allows for precise control of reaction parameters, including temperature, stirring rate, and light intensity. Its unique multi-wavelength LED configuration allows for up to 7 different wavelengths of light, making it ideal for a wide range of photochemical reactions. The reactor is compact and comes with four panels, and it is compatible with both batch and flow reaction setups, making it suitable for use in academic and industrial settings. Its high-intensity LEDs generate light of various wavelengths, and the reaction vessel is made of high-quality borosilicate glass, allowing for exemplary transparency and chemical resistance. The

programmability of the reactor allows for precise control of reaction conditions such as temperature and irradiation time. The PhotoCube reactor has been used for various applications, including the synthesis of new organic compounds, degradation of environmental pollutants, and photovoltaic devices research, among others. In my case, I used the 4-mL glass vials because I was working with a small amount of reagent. (Available batch reactor volumes: 4-mL and 30-mL glass vials).

The cerium(III) chloride salt is readily soluble and dissolves in several solvents, including water, aqueous $HClO_4$, and aqueous H_2SO_4, resulting in transparent mixtures. With these solutions, water-splitting experiments were performed. To improve removal of the gas formed during water-splitting (as well as evaporation) in experiments, holes were introduced on the vial caps, and constant conditions of UV-365 light, 1500 rpm stirring, and four panels were maintained throughout the trials. A gradual increase in temperature was observed during the experiment, reaching a maximum of 32 °C after 33 minutes, starting from 24 °C. I conducted experiments using the PhotoCube photoreactor for one to two hours. During the experiments, I measured the weight of the vials before and after illumination and the weight of the stirring bars and salt added. These measurements were taken every ten minutes.

4. Results and Discussion

4.1. Calibration of the PhotoCube photoreactor using actinometry

Ferrioxalate actinometry[26] is a method for determining the photon flux in a photochemical system. The Fe(II) ion production rate is proportional to the photon flux in the system.

To measure the course of the actinometric reaction (see: Figure 5), a solution containing 650 microlitres of the 0.00106 mol/dm^3 solution of $K_3[Fe(C_2O_4)_3]\cdot 3H_2O$ (crystals with a greenish hue) is mixed with 750 microlitres of 0.50 mol/dm^3 H_2SO_4 and 1150 microlitres of 1.0 mol/dm^3 sodium acetate. The solution is also supplemented with 26 microlitres of 0.050 mol/dm^3 phenanthroline to detect the complex, resulting in a light-yellow colour.

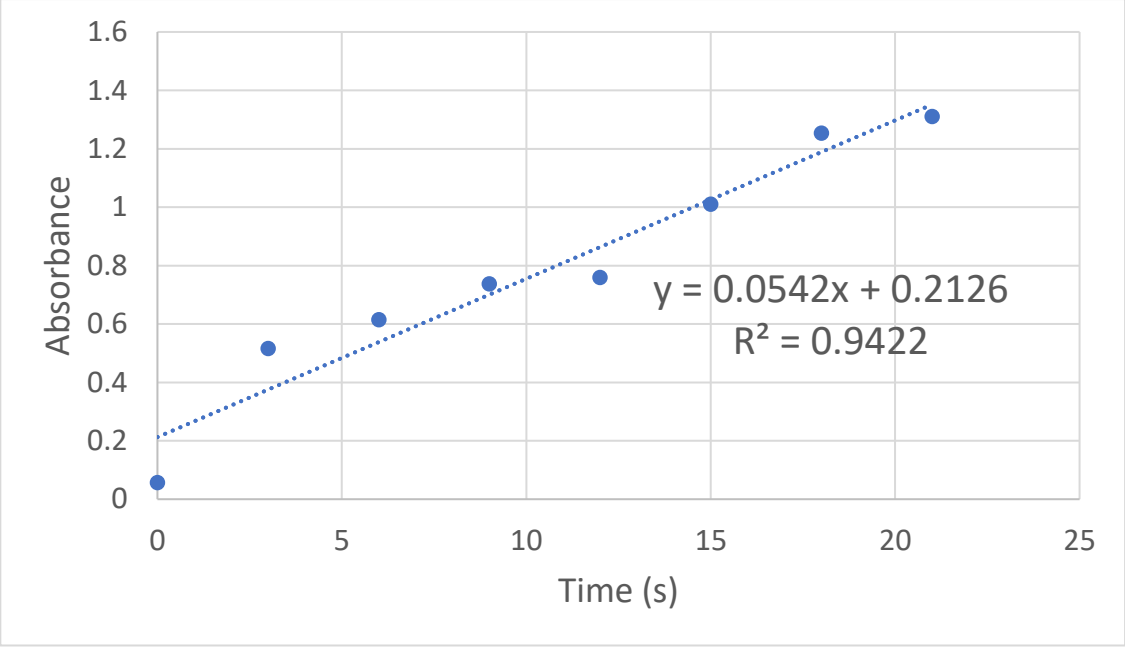

Figure 6: Kinetic curve of potassium-tris(oxalato)-ferrate(III) trihydrate solution after illumination in the PhotoCube photoreactor at different times and detected at 512 nm in the scanning spectrophotometer

The solution was placed in vials, which were illuminated for different times. The first vial was left without illumination (0 seconds), while the second, third, fourth, fifth, sixth, seventh, and eighth vials were illuminated for 3, 6, 9, 12, 15, 18, and 21 seconds, in order. The colour of the complex formed is reddish orange after illumination for a few seconds in the PhotoCube

photoreactor. To detect the complex, absorbance readings at the wavelength of 512 nm were used.

In the PhotoCube reactor, excitation light of several wavelengths (365, 395, 457, 500, 523, 595, 623 nm and white light) can be applied. However, since my purpose was to measure the Ce(III) catalyzed water decomposition, and since Ce(III) absorbs light in the UV range, I performed the calibration of the 365 nm LED. Monochromatic LED light sources have a characteristic half-width of 10-75 nm (typically 20 nm).[31]

The LED power of PhotoCube can be changed up to 128 W for each colour. For actinometric calibration (as well as for the water-splitting experiments later, in **Chapter 4.3.**), 100% power was used.

The equations given in **Chapter 4.2.** were used for the calibration of the PhotoCube photoreactor.

Table 2: Values obtained from equations (1-9) of Chapter 4.2. The quantum yield of the reaction at 365 nm is 1.24.[25] For the photoreactor calibration measurements, the value for ε(epsilon) for the $[Fe(phen)_3]^{2+}$ complex is 11000 $dm^3/mol/cm$.[26] The volume of the sample was 2.5 cm^3.

Total emitted photon energy:	**$6.95 \cdot 10^{-3}$ J/s**
Total number of emitted photons:	$1.28 \cdot 10^{16}$ 1/s
Energy of one single photon with 365 nm ($E = hc/\lambda$):	$5.44 \cdot 10^{-19}$ J
Rate of the decomposition reaction (see: Eq. 6 but at 512 nm instead of 390 nm):	$4.93 \cdot 10^{-6}$ mol/dm^3/s
The slope of the kinetic curve at 512 nm (see: Figure 6):	0.0542 1/s
Fraction of absorbed photons (see: Eq. 2):	46.7 %
Initial absorbance of the actinometer solution at 365 nm:	0.2733

4.2. Calibration of the diode array spectrophotometer

I used UV-visible spectroscopy to study the reaction between Ce(IV) and water, which is known as a photochemical reaction. However, to study a photoreaction in a spectrophotometer, the light intensity calibration of the photometer must be performed since this is not the conventional use of a spectrophotometer.

For the calibration, actinometry was used, but instead of IUPAC actinometry, I used the method specially developed for diode array spectrophotometers by T. Lehóczki.[26] For the measurements, a magnetic stirring was applied. The measurements were performed at room temperature in a 1.00 cm quartz cuvette. I employed an Analytik Jena SPECORD S600 diode array spectrophotometer, which has deuterium and halogen lamp light sources and is controlled by WinASPECT software. Although the spectrum was recorded between 180-1100 nm, I only used the 200-550 nm range for analysis in some cases.

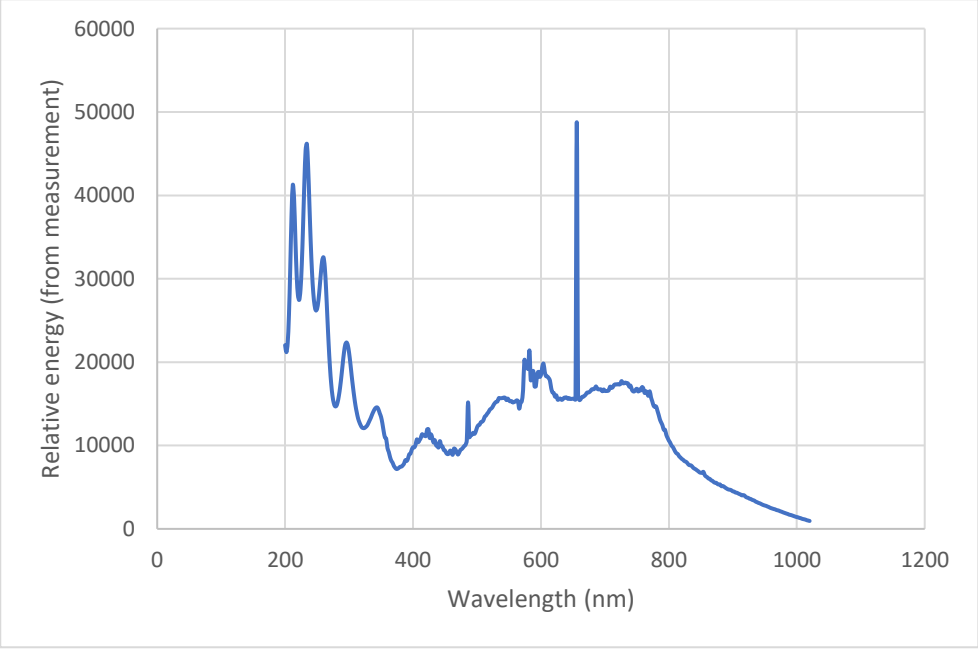

Figure 7: Relative energy spectrum of the Analytik Jena SPECORD S600 diode array spectrophotometer.

The Analytik Jena SPECORD S600 diode array spectrophotometer can record kinetic curves in two ways: to enable the "shutter always open" function, exposing the sample continuously

to the light of the spectrophotometer lamps during both spectra recording and all other times. The other option is to turn off the "shutter always open" function, exposing the sample only to light during spectrum recording time (typically 51 ms/spectrum). The light shutter is closed between two measurements to prevent sample illumination.

I calculated the relative emitted photon number ($N_{\text{photon, rel}}$) as a ratio of the reciprocal of the measured relative energy and its corresponding wavelength value (λ, nm). The relative emitted photon number is unitless.

$$N_{photon,rel} = \frac{E_{rel}}{\frac{1}{\lambda}} = E_{rel} \cdot \lambda \tag{1}$$

Then I calculated the fraction of absorbed photons:

$$\frac{I}{I_0} = 1 - 10^{-V_{sample} \cdot A_0} \tag{2}$$

The sample volume was an important consideration because the UV lamp illuminated the sample from above, meaning that the 1.00 cm path length of the cuvette would differ from the thickness of the layer on which I wanted to determine the quantity of the transmitted light. Since the bottom of the cuvette was 1.00 cm × 1.00 cm, the measured volume of the solution was equal to the thickness of the liquid column, which is the actual path length. Therefore, the "V_{sample}" term in equation (2) represents the sample volume in cubic centimetres without any units of measurement. By multiplying the two previously calculated values, I obtained the relative absorbed photon number ($N_{\text{photon, absorbed}}$) for each measured wavelength.

$$N_{photon,absorbed} = \frac{I}{I_0} \cdot N_{photon,rel} \tag{3}$$

I was able to calculate the amount of relative formed product ($N_{P,\,rel}$) using the relative absorbed photon number and the quantum utilization factor (ϕ) value obtained at the

corresponding wavelength mentioned earlier. The sum of the amount of the relative formed product can be given in equation (5).

$$N_{P,rel} = N_{photon,absorbed} \cdot \phi \tag{4}$$

$$\Sigma\, N_{P,rel} = \Sigma\, N_{photon,absorbed} \cdot \phi \tag{5}$$

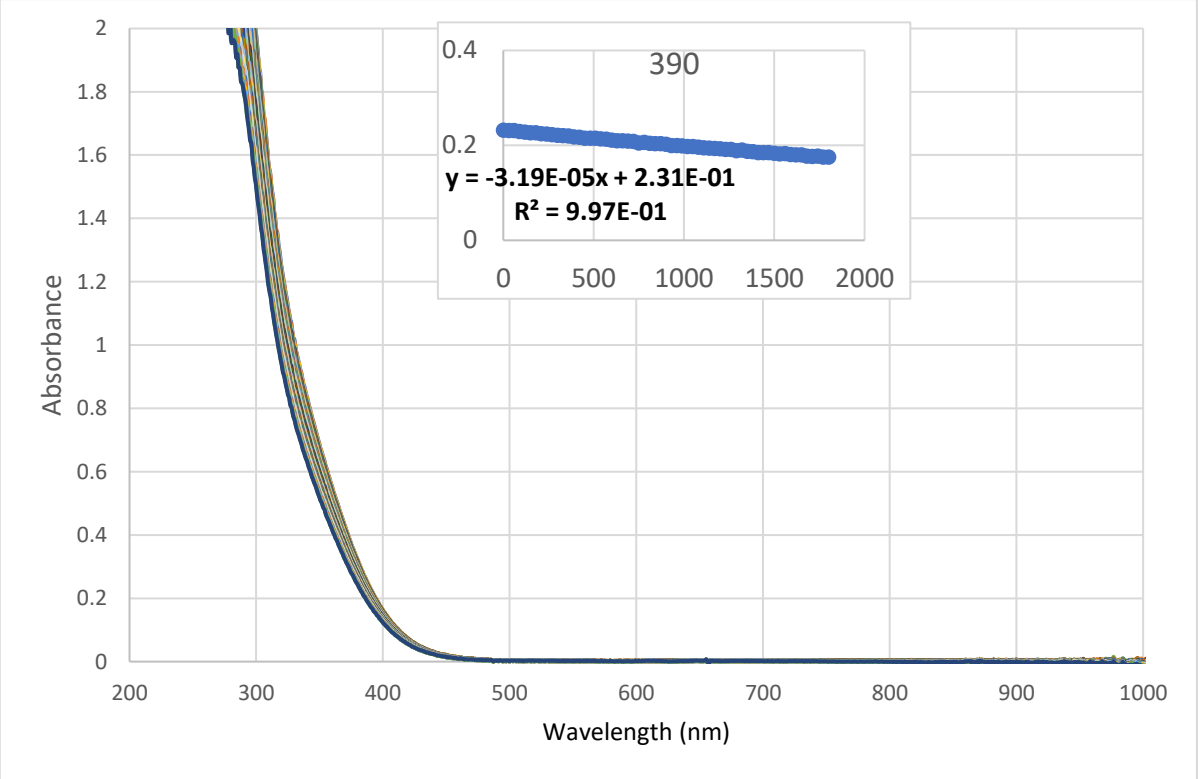

Figure 8: Kinetic curve of potassium-tris(oxalato)-ferrate(III) trihydrate solution at a wavelength of 390 nm, measured in an Analytik Jena SPECORD S600 spectrophotometer. The volume used for each measurement was 2.5 cm^3, and the concentration of the solution was $1.06 \cdot 10^{-3}$ M. The measurement lasted 40min with the spectrum recorded every 30 s.

To determine the absolute concentration of the product formed per second in units of mol/dm^3/s, divide the steepness of the kinetic curve at 390 nm (dA/dt, s^{-1}) by the molar absorptivity (ε(390nm) = 312 dm^3/mol cm) at that specific wavelength. Equation (6) uses ℓ = 1.00 cm.

$$\frac{dc}{dt} = \frac{-\frac{dA}{dt}}{l \cdot \epsilon_{(390nm)}} \tag{6}$$

One can calculate the amount of product formed in the entire sample per unit time ($\sum N_P$, s^{-1}) by taking the product of the absolute concentration of product formed per second (dc in mol/dm3 s) with the sample volume expressed in dm^3 (V_{sample} = 2.5 cm^3), and then multiplying the result by Avogadro's constant ($N_A = 6.022 \cdot 10^{23}$ mol^{-1}).

$$\Sigma\, N_P = \frac{dc}{dt} \cdot N_A \cdot V_{sample} \tag{7}$$

$$N_{photon} = \frac{\Sigma\, N_P}{\Sigma\, N_{P,rel}} \cdot N_{photon,rel} \tag{8}$$

To determine the actual emitted photon number per wavelength (N_{photon}, s^{-1}), I divided the quantity of product formed in the entire sample per unit time ($\sum N_P$, s^{-1}) by the total amount of product formed (relative) ($\sum N_{P,\,rel}$), and then multiplied the result by the relative emitted photon number ($N_{photon,\,rel}$).

To summarize, the actual number of emitted photons per wavelength (N_{photon}, s^{-1}) can be obtained by dividing the quantity of product formed in the entire sample per unit of time ($\sum N_P$, s^{-1}) by the total amount of product formed (relative) ($\sum N_{P,\,rel}$), and multiplying by the relative emitted photon number ($N_{photon,\,rel}$). The energy of each emitted photon per wavelength (E, J/s) can be calculated by multiplying the actual emitted photon number per wavelength with Planck's constant ($h = 6.626 \cdot 10^{-34}$ J s), the speed of light (c = 299792458 m/s), and dividing by the wavelength (λ, m). The total emitted photon number ($\sum N_{photon}$, total photons/s) can be obtained by adding these values.

$$E = N_{photon} \cdot h \cdot \frac{c}{\lambda} \tag{9}$$

Table 3: Using the equations above (1-9) the data in the table contains the calculated results.

Total emitted photon energy:	**$2.45 \cdot 10^{-4}$ J/s**
Total number of emitted photons:	$6.36 \cdot 10^{14}$ 1/s
Rate of the decomposition reaction:	$1.022 \cdot 10^{-7}$ mol/dm^3/s
The slope of the kinetic curve at 390 nm (see: Figure 8):	$-3.19 \cdot 10^{-5}$ 1/s

From the actinometric measurement, not only the total emitted energy of the photons in the 200-1100 nm range, but also the energy distribution of the spectrophotometer lamps can be calculated, and it is shown in Figure 9. We can see that, although the total emitted photon energy of the diode array spectrophotometer is comparable with that of the PhotoCube reactor, in the case of the spectrophotometer, the emitted photon number is quite high at $\lambda > 500$ nm which is ”useless” for driving either the actinometric reaction or the Ce photoreactions. This explains why the actinometric reaction rate is so fast in the PhotoCube.

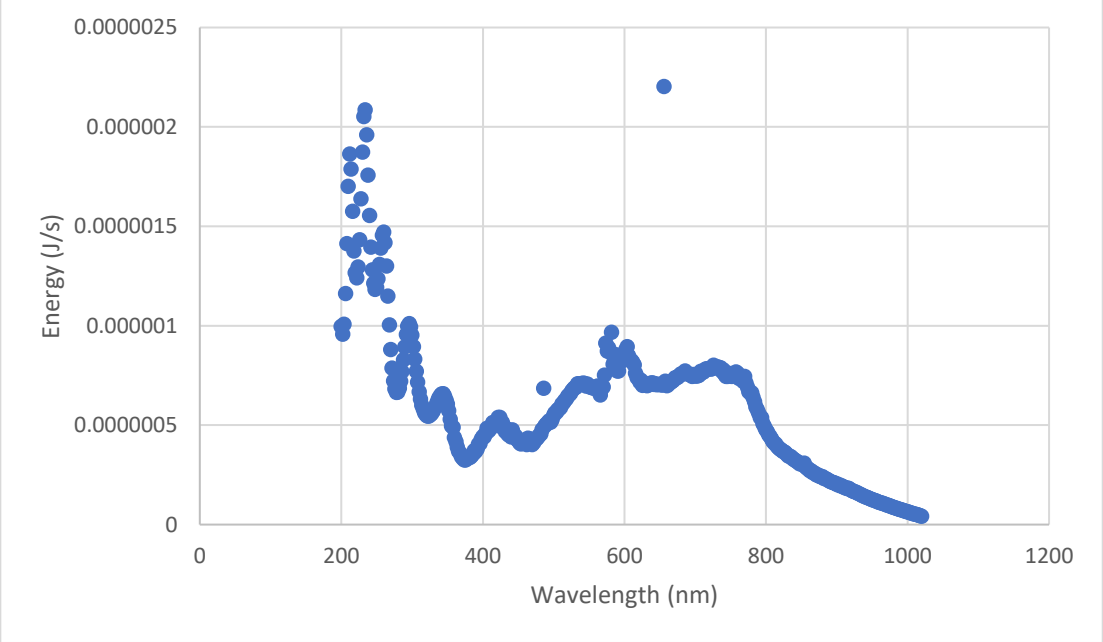

Figure 9: Energy spectrum of the Analytik Jena SPECORD S600 diode array spectrophotometer.

Also, when two spectrophotometers are compared, similar photon flux values are found: the overall photon flux for a spectrophotometer in the paper of T. Lehóczki[26] was $1.7 \cdot 10^{15}$ s^{-1},

which agrees well with the value for our spectrophotometer, which has an overall photon flux = $6.36 \cdot 10^{14}$ 1/s.

4.3. Ce(III) catalyzed water-splitting kinetics in PhotoCube

4.3.1. Reaction with mass measurements

H_2O evaporation has been checked first, as the water was one of the solvents used for this experiment. A few trials have been done, and the following results occurred. For these experiments, I used deionized water. 100% UV illumination and the stirring process were on during the whole process. The volume of the samples was 2.5 cm^3.

The first measurements indicated some experimental difficulties which needed to be solved. First, the temperature of the samples changed substantially during illumination (6 °C increase after 30 minutes). From these preliminary measurements, we concluded that the masses of the samples practically did not change or even increased slightly.

Also, there were some reproducibility problems in the first few experiments. Namely, there was a break point on the kinetic curves (see the orange dots of figure 10). We assumed that this change of slope is coming from the fact that the gas phase of the vial becomes saturated after 35-40 minutes to water vapour.

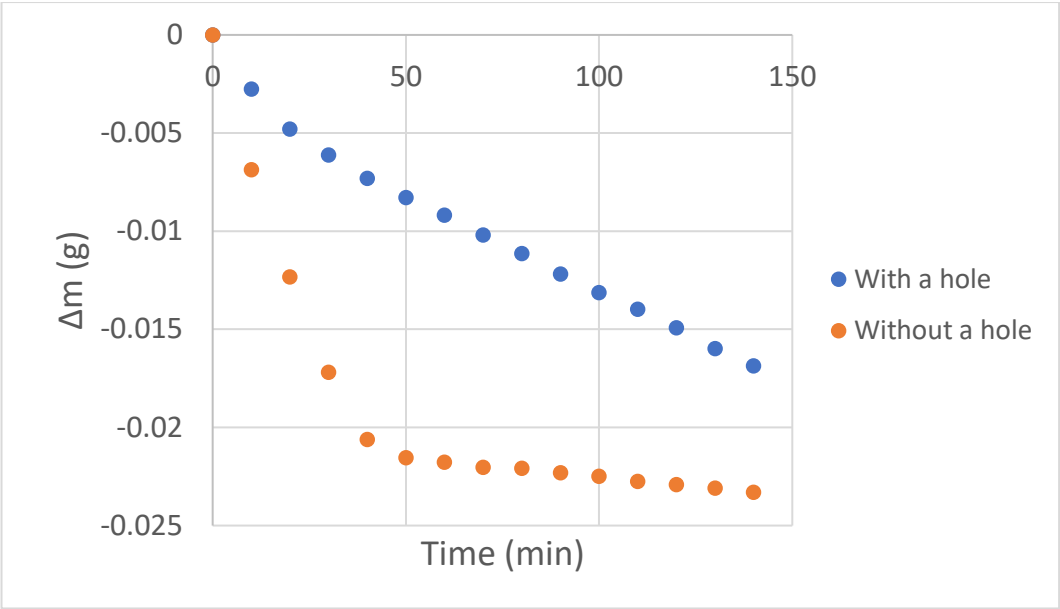

Figure 10: Mass change of water samples during illumination in PhotoCube, with and without a hole on the top of the cap of the glass vial (effect on the evaporation process).

Table 4: SciDAVis fitting results for the illumination of water in PhotoCube.

	Initial slope (g/min)	Chi^2	R^2
With a hole on top of vial	$(-1.32 \pm 0.04)\cdot 10^{-4}$	$2.65\cdot 10^{-5}$	0.99
Without a hole on top	$(-2.28 \pm 0.2)\cdot 10^{-4}$	$6.87\cdot 10^{-4}$	0.88

Before recognizing the importance of placing a hole on the cap of the glass vial, we performed several kinetic measurements with water, perchloric acid, and additional Ce(III) in less and more amounts (for the concentration values, see also Table 1).

In Figure 11, the mass reduction (Δm) over time is depicted for three different solvents with and without the addition of cerium(III). The measurements for water (m00), $HClO_4$ (m11-m13), and H_2SO_4 (m21-m23) are shown. The compositions of the samples is collected in Table 5.

Table 5: Sample preparation and concentration values for the kinetic measurements in $HClO_4$ and H_2SO_4 solutions. The volumes of the stock solution were 500 cm^3.

Medium	Sample symbol	Mass of Cerium(III) used (g):	$c_{Ce(III)}$ (mol/dm^3)
water	**m00**	**0**	**0**
0.9927 mol/dm^3 aqueous $HClO_4$	**m11**	**0**	**0**
	m12	**0.06006**	**$3.22 \cdot 10^{-4}$**
	m13	**0.12317**	**$6.61 \cdot 10^{-4}$**
0.50 mol/dm^3 aqueous H_2SO_4	**m21**	**0**	**0**
	m22	**0.06256**	**$3.35 \cdot 10^{-4}$**
	m23	**0.12437**	**$6.67 \cdot 10^{-4}$**

The most significant decrease in mass is observed in $HClO_4$ (m11), which is the acid solution illuminated without any catalyst. It is also visible, that the break point of all curves is at about 35-40 minutes.

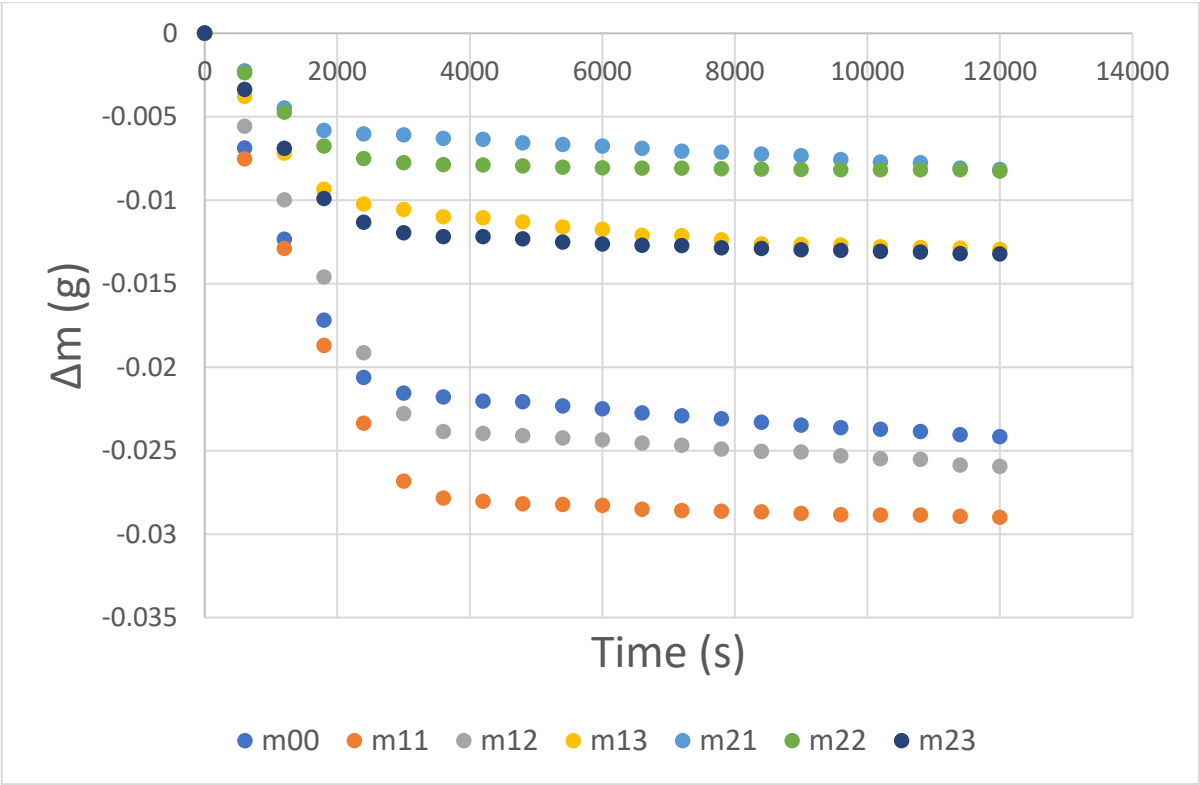

Figure 11: A sum of three experiments-H_2O (m00), H_2SO_4 (m21, m22, m23), and $HClO_4$ (m11, m12, m13) with/without adding cerium ions, illuminated under 100% UV light, and stirred for 3 hours and 20 min (12000s).

The last important conclusion from the preliminary measurements was that instead of the mass values, it is better to use the mass reduction (Δm) values, where $\Delta m = m - m_0$. The Δm values can be compared for parallel measurements even when the initial masses are somewhat different. So, for all presented experiments, I am showing the mass reduction values instead of the measured mass values.

Figure 12: A representation of the glass vials used for PhotoCube measurements with and without a hole on the top of the vial.

For my experiment, I made the initial measured mass of the vial, solution, and Ce(III) subtracted from itself. This ensured that the first values in Table 6 to be always zero. Additionally, I subtracted each subsequent value from the first measured mass (m_0). By performing this procedure, I was able to generate a kinetic curve starting from the zero value on the graph. This representation provides a more enhanced and lucid visualization.

Table 6: An example of one measurement and calculation for mass reduction (Δm) for each vial. These are the first few data plotted on Figure 11.

	m00	m11	m12	m13	m21	m22	m23
0	0	0	0	0	0	0	0
600	-0.00687	-0.00753	-0.00556	-0.00379	-0.00225	-0.00237	-0.00336
1200	-0.01234	-0.0129	-0.00998	-0.00718	-0.00448	-0.00472	-0.00689
1800	0.01719	-0.0187	-0.01459	-0.00934	-0.00581	-0.00676	-0.00991
2400	-0.02062	-0.02336	-0.01914	-0.01023	-0.00603	-0.00751	-0.01132
3000	-0.02155	-0.02682	-0.02279	-0.01055	-0.00608	-0.00775	-0.01196
3600	-0.02178	-0.02785	-0.02386	-0.01099	-0.0063	-0.00787	-0.01218

4.3.2. Effect of changing the Ce(III) concentration

Minor variations can be observed in adding the Ce(III) salt to the same amount of solvent ($HClO_4$). I conducted three parallel measurements for three scenarios: illumination of $HClO_4$ only, adding a smaller amount of cerium(III) salt to $HClO_4$, and adding a more significant amount of cerium(III) salt to $HClO_4$. The results of the parallel measurements are almost perfectly aligned in Figure 13, indicating that the illumination of perchloric acid is reproducible under UV illumination in the PhotoCube.

Table 7: SciDAVis fitting results for the illumination of $HClO_4$ and $HClO_4$ + Ce(III) in PhotoCube.

$c_{Ce(III)}$ (mol/dm^3)	Slope (g/s)	Chi^2	R^2
0	$(-1.05 \pm 0.01)\cdot10^{-4}$	$1.46\cdot10^{-6}$	0.997
$3.11\cdot10^{-4}$	$(-1.25 \pm 0.02)\cdot10^{-4}$	$2.18\cdot10^{-6}$	0.997
$9.21\cdot10^{-4}$	$(-9.1 \pm 0.1)\cdot10^{-6}$	$1.15\cdot10^{-6}$	0.997

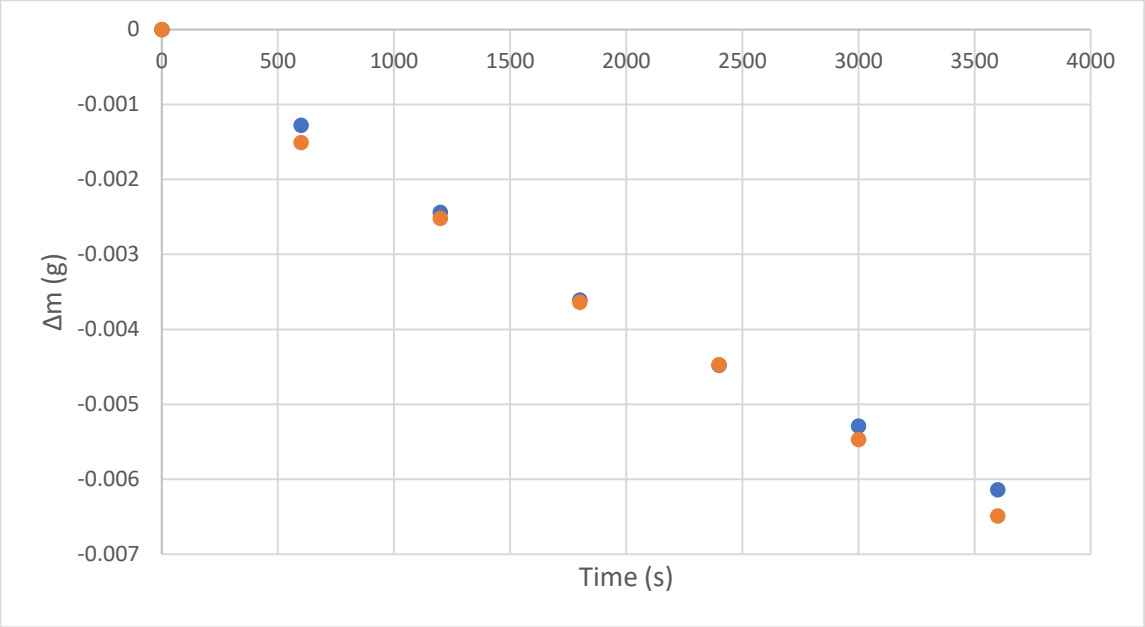

Figure 13: Mass reduction for $HClO_4$ solution in a vial with a hole illuminated for 1 hour with UV light in a PhotoCube photoreactor (two parallel measurements).

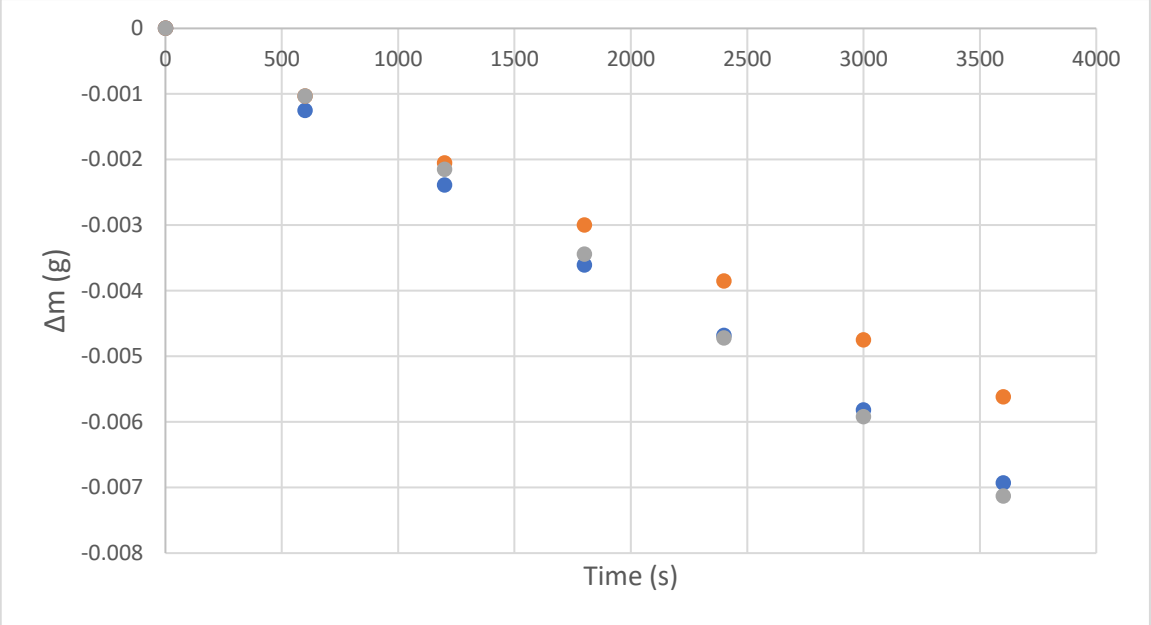

Figure 14: Mass reduction after the addition of Cerium(III) ions in a lower amount to the perchloric acid and illuminating it for 1 hour under UV light in PhotoCube photoreactor using a vial with a hole on the top (three parallel measurements).

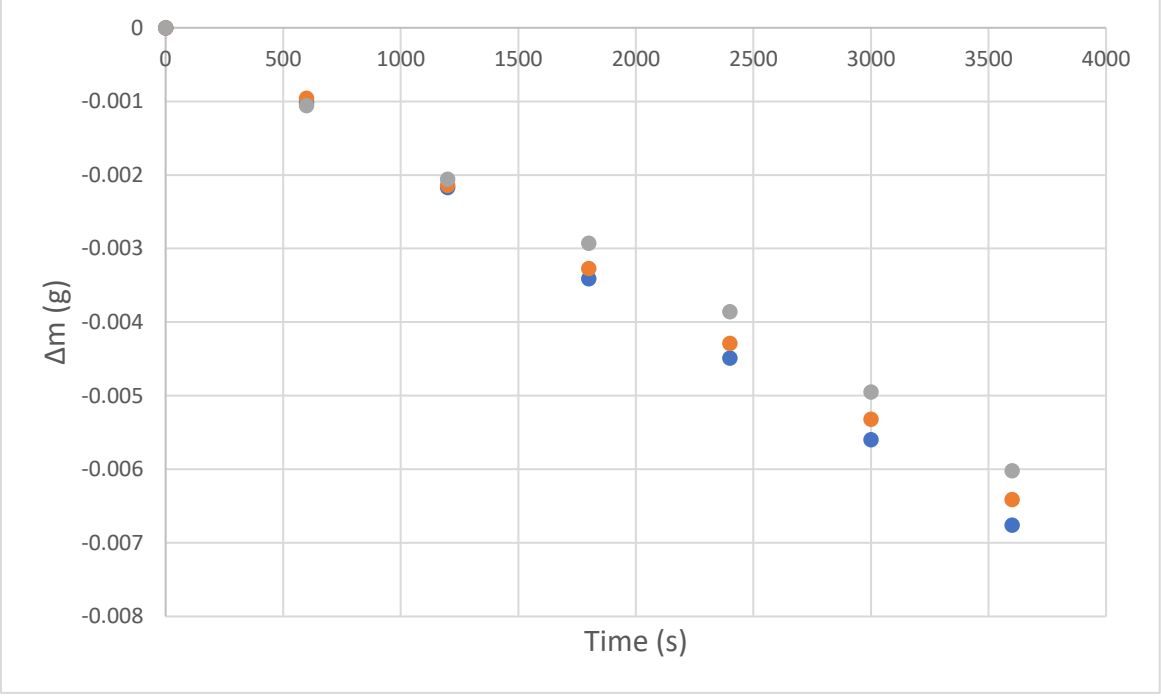

Figure 15: Addition Cerium salt in a higher amount to the perchloric acid solution with illumination for 1 hour under 100% UV light in the PhotoCube photoreactor (three parallel measurements).

As I mentioned earlier, the other experimental problem with the PhotoCube measurements was the increase of temperature during illumination. So, now a thermostat is also connected to the photoreactor to keep the temperature of the sample constant. Although, the photoinitiation step of a photoreaction is typically independent of temperature, there are further thermal steps which can be accelerated by increasing the temperature. So, to achieve full reproducibility, thermostatting is an important issue. Unfortunately, the thermostat was installed after the measurements for my thesis were performed, so I cannot demonstrate the effect of constant temperature here.

4.4. Kinetics of the Ce(IV)+H_2O reaction in the diode array spectrophotometer

To follow the water decomposition reaction, the light intensity of a diode array spectrophotometer is not high enough. This was tested by I. Rapp-Kindner at several different Ce(III) concentrations, and different media (nitric acid and perchloric acid). However, the water oxidation by Ce(IV) is a faster reaction and, when using sulfuric acid as medium, it is readily measurable.[14] So, perchloric acid was also tested in this reaction.

The Ce(IV) sulfate salt was dissolved in $HClO_4$ solution (1 mol/dm^3). The powder dissolves quickly and the solution is very light yellow (almost colourless). To measure its kinetics, I had put the compound in a quartz cuvette and illuminated for 30 minutes in the diode array spectrophotometer, selecting the whole spectrum. Also, we used the “shutter always opened” setup to maximize the illumination intensity. This is the same setup as the one used for actinometric calibration.

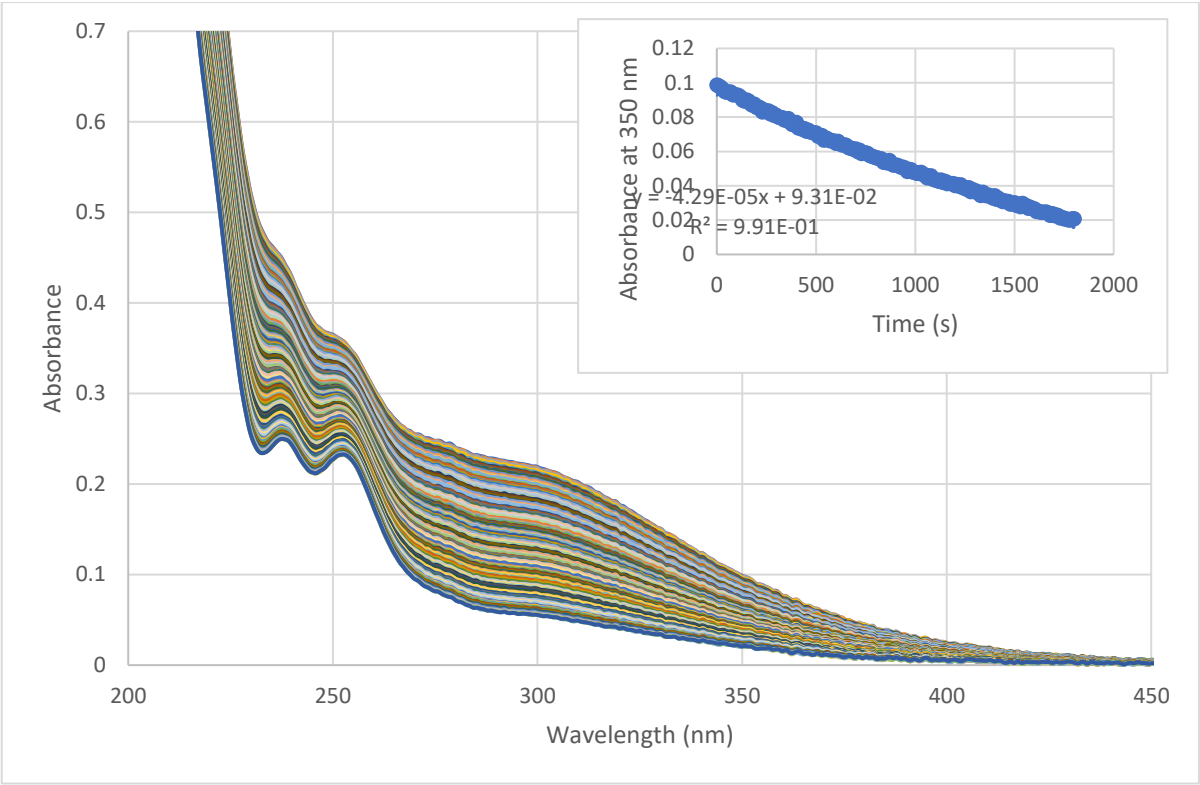

Figure 16: Spectrum of Ce(IV) salt in $HClO_4$ measured in diode array spectrophotometer.

In order to follow the course of this reaction, i.e. to calculate the concentration of the Ce(IV) reagent, I used the Lambert-Beer law. The Beer-Lambert law is widely used in spectrophotometry to determine the concentration of a substance in a solution by measuring its absorbance at a specific wavelength. It assumes a linear relationship between absorbance and concentration if the solution obeys the law, and the concentration is within a certain range.

$$A = \varepsilon c l$$

A	Absorbance	
ε	Molar absorption coefficient	$M^{-1}cm^{-1}$
c	Molar concentration	M
l	optical path length	cm

The initial concentration was set so that the initial absorbance is a well-measurable value at 350 nm. Then, the photochemical reaction between Ce(IV) and water (see: left-hand side half-reaction of the cycle in Figure 2) was detected using multiwavelength detection in the same diode array spectrophotometer which was also used to initiate the reaction. The kinetic curves were evaluated at 350 nm.

From the spectral changes (Figure 16), we can see that after 30 min illumination 80 % of the Ce(IV) is already converted to Ce(III). However, even in the first spectrum, the presence of Ce(III) can be detected, based on the fine structure of the first spectrum in the 230-260 nm range. This indicates that a few minutes of ambient light can cause measureable photoreaction in this system.

The initial rate of the reaction can be calculated based on the initial absorbance change (inset of Figure 16) and the Beer-Lambert law as follows:

$$v = \frac{d[Ce(IV)]}{dt} = \frac{dA}{dt} \cdot \frac{1}{\varepsilon l}$$

This equation is quite similar to Eq. 6. but the parameters are different here.

Table 8: Results from kinetic measurements: measurement conditions and rate of the Ce(IV)+H_2O reaction.

c_{HClO4}	**0.9927 mol/dm^3**
$c_{Ce(IV)}$	$2 \cdot 10^{-4}$ mol/dm^3
l	1.000 cm
Slope of the kinetic curve measured at 350 nm	$-4.29 \cdot 10^{-5}$ s^{-1}
λ (wavelength)	350 nm
ε_λ	633 dm^3/mol/cm
v_0	$6.78 \cdot 10^{-8}$ mol/dm^3/s

Similar measurements were performed by I. Rapp-Kindner and her results are well comparable with my results. In her experiments, the reaction rates scale between $1.9 \cdot 10^{-8}$ mol/dm^3/s and

$7.3 \cdot 10^{-8}$ mol/dm^3/s when changing the concentration of Ce(IV) from $4.0 \cdot 10^{-4}$ mol/dm^3 to $1.4 \cdot 10^{-3}$ mol/dm^3.*

* Unpublished results of Ms. Ildikó Rapp-Kindner.

5. Summary

The production of renewable/solar energy is a key environmental issue nowadays. Photochemical decomposition of water is one of the most promising approached here producing hydrogen. The catalytic process can use cerium(III) ions as catalyst in homogeneous media. In my thesis, I studied the kinetics of the catalytic reaction as well as one of its half-reactions, namely, the redox reaction between water and cerium(IV).

There were two separate experimental tools used to study these reactions. One is a PhotoCube photoreactor with 365 nm monochromatic LED light source. The other one was a diode array spectrophotometer, which also have a light intensity high enough to drive certain photochemical processes. The lamps of this later one is polychromatic, emitting in the entire UV-Vis range.

Before using these two experimental tools to study the water-splitting reaction, a light intensity calibration was performed and the emitted photon flux was determined using potassium-tris(oxalato)-ferrate(III) actinometry. For the PhotoCube, the total emitted photon energy was $6.95 \cdot 10^{-3}$ J/s and the total number of emitted photons was $1.28 \cdot 10^{16}$ 1/s. For the Analytik Jena SPECORD S600 diode array spectrophotometer, the total emitted photon energy was $2.45 \cdot 10^{-4}$ J/s and the total number of emitted photons was $6.36 \cdot 10^{14}$ 1/s.

The water-splitting reaction catalyzed by Ce(III) was measured in aqueous perchloric acid medium in the PhotoCube reactor. Several experimental techniques were tested and the followings are the most important conclusions:

- The use of mass reduction values instead of mass values makes the measurements more comparable.
- The mass reduction happens even without adding Ce(III) or $HClO_4$ to the system. So, evaporation of the solvent cannot be neglected.
- If we want to have reproducible kinetic curves, a hole should be placed on the vial to avoid the formation of saturated gas phase.

- Thermostatting is important for longer kinetic curves since the temperature of the samples increases substantially.

The Ce(IV)+water photo-redox reaction was measured in aqueous perchloric acid medium in the diode array spectrophotometer. This reaction is much faster than the photochemical water-splitting, so, a lower light intensity is enough to drive the reaction. At c_{HClO4} = 0.9927 mol/dm3 and $c_{Ce(IV)}$ = $2 \cdot 10^{-4}$ mol/dm^3, the rate of the reaction is $6.78 \cdot 10^{-8}$ mol/dm^3/s. It means that after 30 minutes of illumination, 80% conversion can be reached. For this light-sensitive reaction, keeping the stock solutions in dark before use is quite important.

6. Acknowledgment

I want to express my heartfelt gratitude to Dr. Katalin Ősz, my supervisor, for igniting my interest in the fascinating field of Photochemistry. Her continuous guidance, mentoring, and support throughout this project have been invaluable, and I am genuinely grateful for her unwavering commitment to my academic and personal development.

I would also like to extend my most profound appreciation to Dr. Gábor Lente, Dr. László Kollár, Dr. Ferenc Kilár, Dr. Attila Felinger, and all other faculty members whose dedication and sincerity in teaching have equipped me with the knowledge and skills necessary to complete this work. I am forever grateful for the wealth of knowledge they have imparted to me, which will undoubtedly benefit me in all aspects of my life.

I want to acknowledge the “Stipendium Hungaricum” program for granting me a full scholarship to pursue my B.Sc. in Chemistry at this university. I am also grateful to my colleagues and friends with whom I have worked during my undergraduate years.

Finally, I am deeply grateful to my mother for her unwavering support and everything she has done for me, which cannot be expressed in words.

7. References

[1] L.J. Heidt, M.E. Smith, Quantum yields of the photochemical reduction of ceric ions by water and evidence for the dimerization of ceric ions, *J. Am. Chem. Soc.* 70 (1948) 2476–2481, https://pubs.acs.org/doi/abs/10.1021/ja01187a050

[2] E. Baur, *Z. physik. Chetn*., 63, 683 (1908), was the first to identify oxygen as the gaseous product of the reaction, https://www.degruyter.com/document/doi/10.1515/zpch-1908-6344/pdf

[3] J. Weiss and D. Porret, *Nature*, 139, 1019 (1937), https://www.nature.com/articles/1391019a0

[4] L. Dogliotti, E. Hayon, Transient species produced in the photochemical decomposition of ceric salts in aqueous solution. Reactivity of nitrogen oxide and hydrogen compd. with oxygen and sulfur (HSO4) free radicals, *J. Phys. Chem*. 71 (1967) 3802–3808, https://pubs.acs.org/doi/abs/10.1021/j100871a014

[5] R.W. Matthews, J. Sworski, Photooxidation and fluorescence of cerium(III) in aqueous sulfuric acid solutions, *J. Phys. Chem*. 79 (1975) 681–686, https://pubs.acs.org/doi/abs/10.1021/j100574a003

[6] R.A. Sheldon, J.K. Kochi, Photochemical and thermal reduction of cerium(IV) carboxylates. Formation and oxidation of alkyl radicals, *J. Am. Chem. Soc*. 90 (1968) 6688–6698, https://pubs.acs.org/doi/abs/10.1021/ja01026a022

[7] D. Greatorex, T.J. Kemp, Electron spin resonance studies of photo-oxidation by metal ions in rigid media at low temperatures. Part 1. Ce(IV) photo-oxidation of alcohols, Transact. *Faraday Soc*. 67 (1971) 56–66, https://pubs.rsc.org/en/content/articlelanding/1971/TF/TF9716700056

[8] D. Greatorex, T.J. Kemp, Electron spin resonance studies of photo-oxidation by metal ions in rigid media at low temperatures. Part 3. Ce(IV) photo-oxidations of aldehydes, ketones, esters and amides, *J. Chem. Soc*. Faraday Trans. 68 (1972) 121–129, https://doi.org/10.1039/F19726800121.

[9] I. Kerezsi, G. Lente, I. Fabian, Highly Efficient Photoinitiation in the Cerium(III)-Catalyzed Aqueous Autoxidation of Sulfur(IV). An Example of Comprehensive Evaluation of Photoinduced Chain Reactions, J. Am. Chem. Soc. 127 (2005) 4785–4793, https://pubs.acs.org/doi/10.1021/ja0439120

[10] G. Lente, J. Kalmar, Z. Baranyai, A. Kun, I. Kek, D. Bajusz, M. Takacs, L. Veres, I. Fabian, One vs. Two-Electron Oxidation with Peroxomonosulfate Ion: Reactions with

Iron (II), Vanadium(IV), Halide ions, and Photoreaction with Cerium(III), *Inorg. Chem*. 48 (2009) 1763–1773, https://pubs.acs.org/doi/10.1021/ic801569k

[11] T.O. Shekunova, L.A. Lapkina, A.B. Shcherbakov, I.N. Meshkov, V.K. Ivanov, A.Y. Tsivadze, Y.G. Gorbunova, Deactivation of singlet oxygen by cerium oxide nanoparticles, *J. Photochem. Photobiol. A: Chem.* 382 (2019) 111925, https://www.sciencedirect.com/science/article/pii/S1010603019301261?via%3Dihub

[12] V.K. Klochkov, Yu.V. Malyukin, G.V. Grygorova, O.O. Sedyh, N.S. Kavok, V. V. Seminko, V.P. Semynozhenko, Oxidation-reduction processes in CeO2-x nanocrystals under UV irradiation, *J. Photochem. Photobiol. A: Chem*. 364 (2018) 282–287, https://www.sciencedirect.com/science/article/pii/S1010603018304726?via%3Dihub

[13] A.R. Soleymani, M. Moradi, Performance and modelling of UV/persulfate/Ce(IV) process as a dual oxidant photochemical treatment system: kinetic study and operating cost estimation, *Chem. Eng. J*. 347 (2018) 243–251, https://www.sciencedirect.com/science/article/pii/S1385894718306697?via%3Dihub

[14] J. Michnyóczki, V. Kiss, K. Ősz, A kinetic study of the photooxidation of water by aqueous cerium(IV) in sulfuric acid using a diode array spectrophotometer, *Journal of Photochemistry and Photobiology A: Chemistry* 408 (2021) 113110. https://doi.org/10.1016/j.jphotochem.2020.113110

[15] M.G. Evans, N. Uri, Photo-oxidation of water by ceric ions, *Nature* 166 (1950) 602–603, https://www.nature.com/articles/166602b0

[16] L. J. Heidt and A. F. McMillan, Influence of Perchloric Acid and Cerous Perchlorate upon the Photochemical Oxidation of Cerous to Ceric Perchlorate in Dilute Aqueous Perchloric Acid, J. *Am. Soc.* 76 (1954) 2135-2139, https://pubs.acs.org/doi/abs/10.1021/ja01637a028

[17] S.Y. Min, T.S. Kim, B.J. Kim, H. Cho, Y.Y. Noh, H. Yang, J.H. Cho, T.W. Lee, Large-scale organic nanowire lithography and electronics, *Nature Communications* 4 (2013) 1773, https://www.nature.com/articles/ncomms2785

[18] P. Arunachalam, A.M.A. Mayouf, Photoelectrochemical Water-splitting, *Noble Metal-Metal Oxide Hybrid Nanoparticles* (2019) 585-606, https://www.sciencedirect.com/science/article/pii/B9780128141342000280

[19] N. A. Piro, J. R. Robinson, P. J. Walsh, E. J. Schelter, The electrochemical behaviour of cerium(III/IV) complexes: Thermodynamics, kinetics, and applications in synthesis 260 (2014) 21-36, https://www.sciencedirect.com/science/article/pii/S0010854513001896

[20] L.F. Arenas, C. Ponce de León, F.C. Walsh, Electrochemical redox processes involving soluble cerium species, *Electochimica Acta* 205 (2016) 226-247, https://www.sciencedirect.com/science/article/pii/S0013468616308611?via%3Dihub

[21] M. Melchionna, A. Trovarelli, P. Fornasiero, Synthesis and properties of cerium oxide-based materials, Cerium Oxide (CeO_2): Synthesis, Properties, and Applications (2020) 13-43, https://www.sciencedirect.com/science/article/pii/B9780128156612000025

[22] K. Binnemans, Chapter 229 Applications of tetravalent cerium compounds, *Handbook on the Physics and Chemistry of Rare Earths* 36 (2006) 281-392, https://www.sciencedirect.com/science/article/abs/pii/S0168127306360035?via%3Dihub

[23] J. R. Bolton, I. M.-Smith, K. G. Linden, Rethinking the Concepts of Fluence (UV Dose) and Fluence Rate: The Importance of Photon-based Units – A Systemic Review, *Photochemistry, and Photobiology* 91 (2015), https://doi.org/10.1111/php.12512

[24] J. Rabani, H. Mamane, D. Pousty, J. R. Bolton, Practical Chemical Actinometry—A Review, *Photochemistry and Photobiology* 97 (2021), https://doi.org/10.1111/php.13429

[25] C. G. Hatchard, C. A. Parker, A new sensitive chemical actinometer - II. Potassium ferrioxalate as a standard chemical actinometer, *Royal Society* 235 1203 (1956), https://royalsocietypublishing.org/doi/10.1098/rspa.1956.0102

[26] T. Lehóczki, É. Józsa, K. Ősz, Ferrioxalate actinometry with online spectrophotometric detection, *Journal of Photochemistry and Photobiology A: Chemistry* 251 (2013) 63-68, https://doi.org/10.1016/j.jphotochem.2012.10.005

[27] A. Gelman, B. Goodrich, J. Gabry, A. Vehtari, R-squared for Bayesian regression models, *The American Statistician* 73(3):1-6 (2018), http://www.stat.columbia.edu/~gelman/research/unpublished/bayes_R2.pdf

[28] J. Kwasiborski, M. Sobol, The chi-square independence test and its application in the clinical researches, *Kardiochirurgia i Torakochirurgia Polska* 4 550–554 (2011), file:///C:/Users/AMPC/Downloads/KiTP_Art_18011-10.pdf

[29] A. Mokeddem, S. Benykhlef, A. A. Bendaoudi 1, N. Boudouaia, H. Mahmoudi, Z. Bengharez, S.D.Topel, Ö. Topel, Sodium Alginate-Based Composite Films for Effective Removal of Congo Red and Coralene Dark Red 2B Dyes: Kinetic, Isotherm and Thermodynamic Analysis, *Water* 15 1709 (2023), https://doi.org/10.3390/w15091709

[30] I. Fabian, G. Lente, Light-induced multistep redox reactions: the diode array spectrophotometer as a photoreactor, *Pure Appl. Chem.* 82 (2010) 1957–1973, https://www.degruyter.com/document/doi/10.1351/PAC-CON-09-11-16/html

[31] C. Dietlin, S. Schweizer, P. Xiao, J. Zhang, F. Morlet-Savary, B. Graff, J.-P. Fouassier, J. Lalevée, Photopolymerization upon LEDs: new photoinitiating systems and strategies, *Polym. Chem.* 6 (2015) 3895–3912, https://pubs.rsc.org/en/content/articlelanding/2015/py/c5py00258c

UNIVERSITY OF PÉCS

Faculty of Sciences
Instituion ID FI58544

Declaration of Originality

Student's Name: Simona Januova

Neptun code: FH8WLY

Title of Thesis: Photochemical water splitting reaction catalyzed by Ce(III) ions

Hereby, I, a student of the Faculty of Sciences at the University of Pécs, in full knowledge of my liability, declare that this thesis is **my own original work.** I have clearly referenced all sources (both from printed and electronic sources) in the text in accordance with international requirements of copyright.

I acknowledge that it is considered plagiarism

- to cite verbatim without using quotation marks and crediting the author
- to paraphrase the source material without citing the source
- to indicate another author's published ideas as my own.

I declare that I have understood the definition of plagiarism and I accept that if my thesis violates copyrights, its assessment shall be fail (1), and the major director of the program shall initiate a disciplinary procedure in front of the Dean according to Article 59 (14) of the Code of Studies and Examinations of the University of Pécs.

Pécs, 15 day, 05 month, 2023 year

signed by student